Acceleration of Fracture Healing by Overexpression of Basic Fibroblast Growth Factor in the Mesenchymal Stromal Cells

HONGLIANG ZHANG,[a,b] ALEXANDER KOT,[a] YU-AN E. LAY,[a] FERNANDO A. FIERRO (ID),[c] HAIYAN CHEN,[a,d] NANCY E. LANE,[a] WEI YAO (ID)[a]

Key Words. Mesenchymal stromal cells • Basic fibroblast growth factor • Osteoblasts • Callus • Bone strength

[a]Center for Musculoskeletal Health, Department of Internal Medicine, [c]Stem Cell Program, UC Davis Health System, Institute for Regenerative Cures, University of California Davis Medical Center, Sacramento, California, USA; [b]Department of Emergency Medicine, Center for Difficult Diagnoses and Rare Diseases, Second Xiangya Hospital of the Central-South University, Hunan, Changsha, People's Republic of China; [d]Adult Programs Division, California Department of Social Services, Sacramento, California, USA

Correspondence: Wei Yao, M.D., Center for Musculoskeletal Health, 4625 2nd Avenue, Sacramento, California 95817, USA. Telephone: (916)-734-0763; Fax: (916)-734-4773; e-mail: yao@ucdavis.edu

ABSTRACT

In this study, we engineered mesenchymal stem cells (MSCs) to over-express basic fibroblast growth factor (bFGF) and evaluated its effects on fracture healing. Adipose-derived mouse MSCs were transduced to express bFGF and green fluorescence protein (ADSC^{bFGF}-GFP). Closed-femoral fractures were performed with osterix-mCherry reporter mice of both sexes. The mice received 3 × 10^5 ADSCs transfected with control vector or *bFGF* via intramuscular injection within or around the fracture sites. Mice were euthanized at days 7, 14, and 35 to monitor MSC engraftment, osteogenic differentiation, callus formation, and bone strength. Compared to ADSC culture alone, ADSC^{bFGF} increased bFGF expression and higher levels of bFGF and vascular endothelial growth factor (VEGF) in the culture supernatant for up to 14 days. ADSC^{bFGF} treatment increased GFP-labeled MSCs at the fracture gaps and these cells were incorporated into the newly formed callus. quantitative reverse transcription polymerase chain reaction (qRT-PCR) from the callus revealed a 2- to 12-fold increase in the expression of genes associated with nervous system regeneration, angiogenesis, and matrix formation. Compared to the control, ADSC^{bFGF} treatment increased VEGF expression at the periosteal region of the callus, remodeling of collagen into mineralized callus and bone strength. In summary, MSC^{bFGF} accelerated fracture healing by increasing the production of growth factors that stimulated angiogenesis and differentiation of MSCs to osteoblasts that formed new bone and accelerated fracture repair. This novel treatment may reduce the time required for fracture healing. STEM CELLS TRANSLATIONAL MEDICINE 2017;6:1880–1893

SIGNIFICANCE STATEMENT

Mesenchymal stem cells engineered to express basic fibroblast growth factor may provide a cell-based treatment for fracture repair that provides an environment rich in stem cells, growth factors, and bone matrix proteins over a short time, thereby promoting bone regeneration.

INTRODUCTION

Traumatic fractures often require hospitalization, surgery, frequent physician visits, and lost time from work. By 2050, the worldwide incidence of hip fractures is projected to increase by 310% in men and 240% in women. The combined lifetime risk for hip, forearm, and vertebral fractures is about 40%, which is equivalent to the risk for cardiovascular disease (quote from International Osteoporosis Foundation). The one-year mortality rate for hip fracture ranges from 12% to 37% and approximately half of patients are unable to regain their ability to live independently. More than 1,200 hip fracture surgeries are performed in the Department of Veteran Affairs hospitals each year and very few veterans (<1%) hospitalized for hip fractures were discharged for home health care [1]. The morbidity associated with hip fractures is high and an effective treatment to accelerate fracture healing is still lacking.

Although there are a handful of methods to chemically enhance the fracture healing process, they have serious limitations. The efficacy of parathyroid hormone (PTH) for fracture healing has been evaluated in rodents [2–4] and recombinant human PTH 1-34 (teriparatide) has been used off-label in clinical practice [5–7]. However, teriparatide has not been approved by the FDA for this indication. Infusions with recombinant human bone morphogenetic proteins (rhBMP) 2 and 7 have been used to treat open tibia shaft fractures and long bone non-unions, but the efficacy of these treatments remains controversial [8–14]. Moreover, rhBMPs have been associated with several side effects, such as inflammation, ectopic

bone formation, tumorigenesis, and the development of antibodies against rhBMPs [11, 15–18]. Thus, there is still an unmet medical need to treat fractures and shorten the time for bone healing.

There are many growth factors that are secreted in response to a fracture. Among these growth factors, RNA and protein levels of basic fibroblast growth factor (bFGF) are significantly elevated in the callus region in rodent fracture models compared to control animals [19–23]. Mice overexpressing bFGF had higher levels of osteoblast maturation and vascular invasion during the early fracture repair period [24]. Previous studies have demonstrated that short-term bFGF injection induces profound de novo bone formation [25, 26]. bFGF stimulates blood vessel growth and has synergistic effects with vascular endothelial growth factor (VEGF) or platelet-derived growth factor (PDGF), which are important angiogenic factors for wound healing [27]. Like BMPs, bFGF can be directly injected or loaded in scaffolds for fracture healing [28–31]. Although injections with bFGF typically increase early osteoprogenitor cell proliferation, stimulate bone formation, and induce larger callus formation compared with controls, it is not known if the treatment improves bone mechanical strength [22, 32–34].

Prolonged exposure to protein mitogens, including bFGF, is associated with increased risk for cancer [35–37]. Moreover, systemic bFGF injection was associated with severe anemia and shifts in the fate of progenitor cells toward the osteoblast lineage at the expense of the hematopoietic lineage, thereby limiting the systemic application of this growth factor [38–40]. Transplantation of mesenchymal stromal cells (MSCs) was found to be more likely to enhance bone and cartilage regeneration when these cells were engineered to express growth factors such as insulin growth factor-1 (IGF-1), bone morphogenetic proteins (BMPs), or VEGF [41–43]. These findings support the use of MSCs as "factories" to produce a sustained local release of low levels of growth factors over a controlled period for injury repair. We hypothesize that the combination of gene and cell therapies would accelerate fracture repair through a combination of both autocrine and paracrine mechanisms, and may be more effective than individual growth factors given systemically.

MATERIALS AND METHODS

Mice and Treatments

Osterix-mCherry (Osx-mCherry) reporter mice were obtained via MTA agreement from Dr. Peter Maye at the University of Connecticut Health Center. Both male and female mice were used as host mice for fractures. Collagen1-green fluorescent protein (GFP) mice (B6. Cg-Tg(Col1a*2.3-GFP)1Rowe/J, Stock 013134), Collagen2-CreERT mice (FVB-Tg(Col2a1-cre-ERT) KA3Smac/J, Stock 006774), and Ai9 reporter mice (B6; 129S6-Gt(ROSA)26Sortm1(Notch1) Dam/J, Stock 007905) were purchased from Jackson Laboratories. Closed transverse diaphysis fractures of the right femur were generated in 2-month-old mice using a previously described method with some modification [44, 45]. Briefly, a 0.38-mm-diameter stainless-steel pin was inserted into the medullary canal. Fractures were created at the mid-femur using a drop-weight blunt guillotine device. Because MSCs given intravenously are likely to be trapped in the lung and very few make it to the systemic circulation, we used intramuscular (IM) injection to bypass the risk of lung embolism. ADSCs or ADSCs^{bFGF} were given at 3×10^5, IM adjacent to the fracture site, at of the same day as fracture operation. Groups of mice from both sexes were euthanized at days 7,

14, 21, and 35 post-fracture. Mice in day 7 group received luciferin injection at 200 mg/mouse (PerkinElmer, Billerica, MA, http://www.perkinelmer.com/). Calcein injection (10 mg/kg) was given to mice in days 21 and 35 groups at -6 and -1 days prior to euthanization. Mice were housed in the animal facility under closely controlled environmental conditions (12-hour light/dark cycle, room temperature 22°C), and fed ad libitum (food and water). The Institutional Animal Care and Use Committee of the University of California Davis approved the animal protocols for surgery, pain relief, and treatments.

MSC Isolation and Culture

Adipose tissue was collected from the abdominal and inguinal regions from wild type (WT) mice, incubated with 0.1% type I collagenase solution in a 195-rpm shaker at 37°C for 90 minutes, centrifuged at 300g for 5 minutes, shaken vigorously for 15 seconds and centrifuged at 300g for an additional 5 minutes at room temperature. The dark cell pellets were collected, suspended in phosphate buffer saline (PBS) containing 10% bovine serum albumin (BSA) and centrifuged at 300g for 5 minutes. The cell pellets were then suspended in cold 1× Magcellect plus via a negative selection principle (CD45-, TER119-; EasySep Mouse Mesenchymal Stem/Progenitor Cell Enrichment Kit, Stem Cell Technologies, Vancouver, Canada, https://www.stemcell.com/). The cells were maintained in Mesencult mouse MSC proliferation medium (Stem Cell Technologies Inc., Vancouver, BC, Canada, https://www.stemcell.com/) and used at passage 2. These cells were 99.99% CD45 negative and positive for CD105 (>70%), CD29 (>99%) and Sca1 (>98%) [46].

bFGF Vectors and MSC Transduction

MSCs were cultured to 70% confluence and subsequently transduced with *bFGF (MNDU3-FGF2-LUC-PGK-EGFP-WPRE)* or control vector. The MSCs were transduced with 20 μg/ml of protamine sulfate. The volume of lentivirus used for each transduction was determined by titration as the required volume to generate approximately 50% GFP-positive MSCs.

MicroCT Scan for Evaluation of Callus

The protocol was designed to reflect variations in callus mineralization during fracture [47]. Briefly, the right distal femurs were scanned with μCT (VivaCT 40, Scanco Medical AG, Bassersdorf, Switzerland, http://www.scanco.ch) at 55 KeV and 145 μA at an isotropic resolution of 10.5 μm in all three dimensions with an integration time of 350 ms. The entire callus was scanned. The outer boundary of the callus was manually defined through contouring and measured at a fixed length of 4 mm covering the full length of the callus. Gaussian filtering with Sigma 1.2 and Support 2 was used to minimize image noise. We used different thresholds to separate new bone and calcified cartilage (250–350) from the well-mineralized cortical bone (350–800) or under-mineralized tissue (<250). The same settings and thresholds were used for all samples.

Cell Counts and Bone Histomorphometry

Mouse samples were embedded in optimum cutting temperature (OCT) for cryosections. Bone histomorphometry was performed on the entire callus, including measurements of total single-labeled and doubled-labeled bone surfaces (Bioquant Osteo 2015, Bioquant, Nashville, TN, http://bioquant.com/). Mineralized surface (MS/BS), mineral apposition rate (MAR), and bone formation rate (BFR/BS) were calculated following recommendations of the
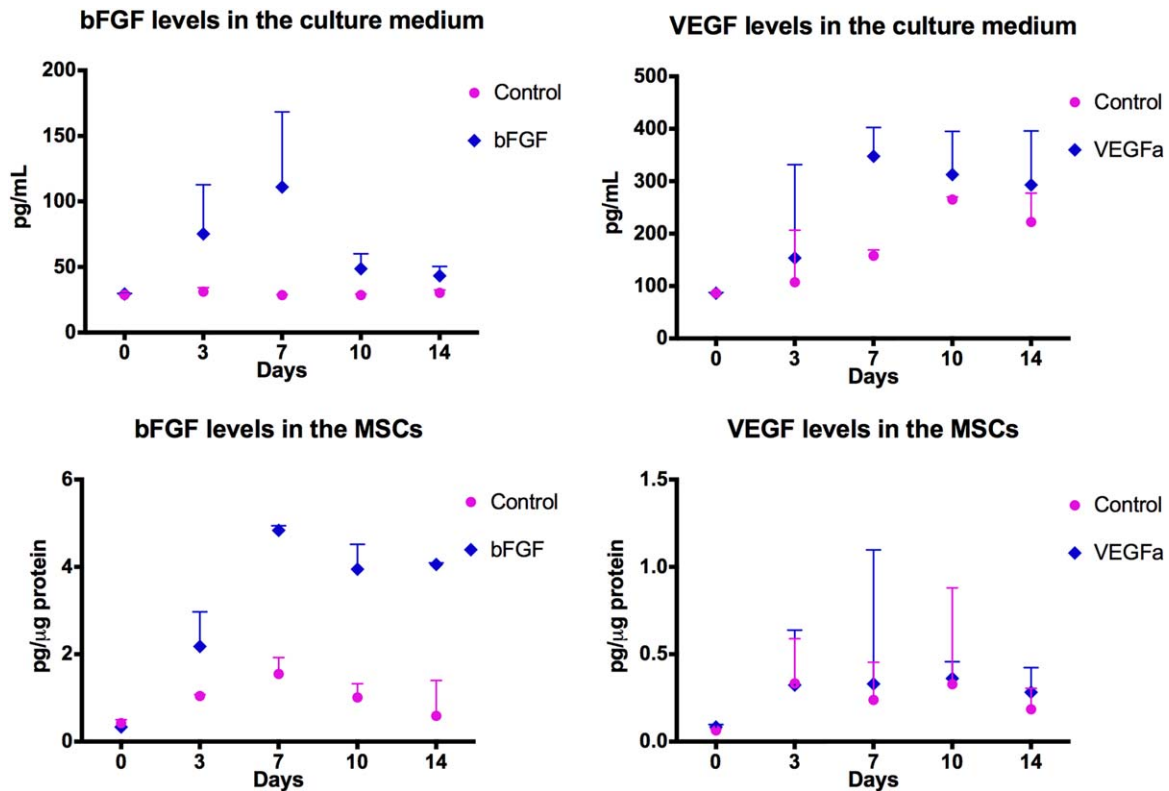
Figure 1

Figure 1. bFGF levels in MSCs and culture supernatant. Adipose-derived mouse MSCs were transduced with bFGF or control vectors and grown to 60% confluence at P0. bFGF and VEGF levels were measured by enzyme-linked immunosorbent assay (ELISA) at days 3, 7, 10, and 14 post-bFGF transduction in both cell lysates and culture medium. Abbreviations: bFGF, basic fibroblast growth factor; MSCs, mesenchymal stromal cells; VEGF, vascular endothelial growth factor.

American Society for Bone and Mineral Research [48]. Cell counts were performed using Keyence cell count software (Keyence BZ-X700 all-in-one fluorescence microscope, Elmwood Park, NJ, http://www.keyence.com),

Immunohistochemistry

Immunohistochemically staining was performed on frozen callus sections using anti-mouse rabbit αSMA VEGF and PDGF-BB antibodies (1:200 to 1:50 dilution, respectively, Abcam, Cambridge, MA, http://www.abcam.com/). Alexa-Fluor 388 0r 594-conjugated secondary antibody were used (1:1,000, Vector laboratories, INC, Burlingame, CA). 4′,6-diamidino-2-phenylindole (DAPI) solution (1:5,000, Vector laboratories, INC, Burlingame, CA, https://vector-labs.com) was applied for 5 minutes for nuclear staining.

Bone Strength Measurement

Each femur was loaded to failure along its long axis using an MTS 831 electro-servo-hydraulic testing system (MTS Systems Corp., Eden Prairie, MN, http://www.mts.com) at a displacement rate of 0.01 mm/second with a 90 N load cell. Sample loads and displacements were continuously recorded throughout each test. Maximum load was determined from the load-displacement curve and the work to fracture was calculated from the area under the load-displacement curve [39, 49, 50].

Statistical Methods

All data are presented as mean ± SD. Null hypothesis testing was performed at a significance level of 0.05. Our primary endpoints

for these studies were callus volume and strength. At each time point, we used the Kruskal–Wallis test to compare the population mean of the outcome variable of interest among all groups. If the overall test was statistically significant, we made pair-wise comparisons to determine which groups were significantly different with the Wilcoxon ranked-sum test. Interactions between sex and treatment within each outcome measurement were evaluated by two-way analysis of variance (ANOVA) (sex, treatment, and their interaction) [46, 51].

ADSC^{bFGF} Exhibited Higher Intracellular and Extracellular bFGF and VEGF Levels

At day 3, bFGF level was increased by twofold increase in ADSC^{bFGF} superman at days 3–7 as compared to control ADSC superannuant. VEGF levels were increased in the culture supernatant starting from day 7 in both the ADSC^{bFGF} and control ADSCs, with higher levels being observed in the ADSC^{bFGF} group. ADSC^{bFGF} had higher intracellular bFGF levels starting from days 3 to days 14, but we did not detect any difference in intracellular VEGF (Fig. 1)

Engraftment of ADSC^{bFGF} in the Callus

Osterix is a marker of osteoprogenitor cells that eventually differentiate into chondrocytes and osteoblasts involved in both endochondral and intramembranous bone formation during fracture healing [52–54]. We used ADSCs from Osx-mCherry mice as donor
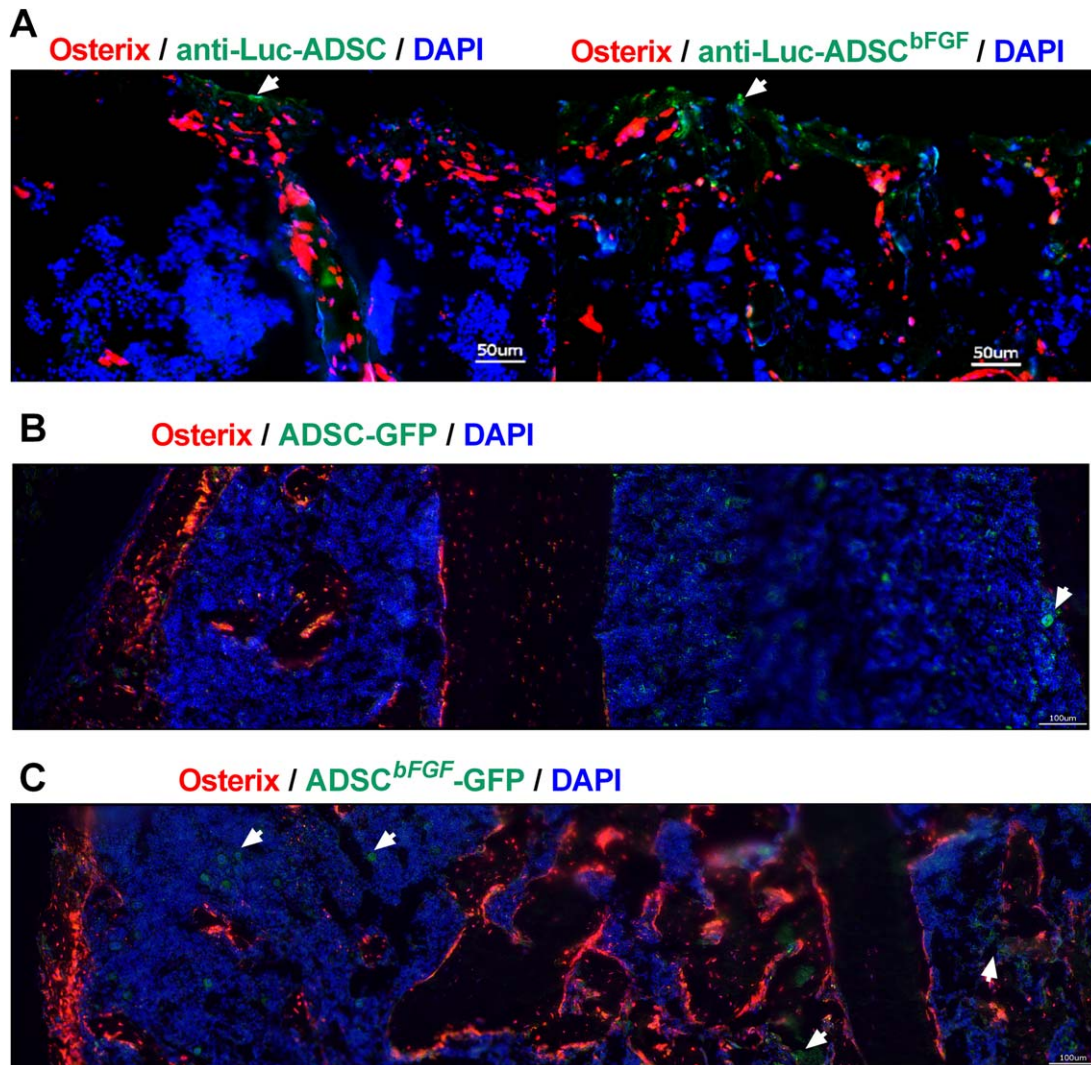
Figure 2. Engraftment of transplanted MSCs in fracture callus at days 14 and 21 post-fracture and cell transplantations. Closed-femoral fractures were performed in the right femurs of 2-month-old female osterix-mcherry mice. These mice received 3×10^5 ADSCs transfected with control vector or ADSC^{bFGF} via IM injection adjacent to fracture sites. **(A)**: Mice were sacrificed at day 14 post-fracture. They were injected with 100 μl of 20mg/mL D-Luciferin Firefly 10 minutes prior to sacrifice. Frozen sections of callus were stained with anti-luciferase antibody followed by Alexa-Fluo 488-conjugated secondary antibody. Scale bar 50 μm. Mice were sacrificed at day 21. Some transplanted cells (in green) were retained in the bone marrow space within the callus (white arrows) in ADSC **(B)** or ADSC^{bFGF} **(C)** treated groups. Scale bar 100 μm. Abbreviations: ADSC, Adipose-derived mouse MSCs; DAPI, 4′,6-diamidino-2-phenylindole; GFP, green fluorescent protein; Luc, luciferase.

cells for transplantation. To visualize the engraftment of ADSCs in bone, femurs of 2-month-old Osx-mCherry mice were fractured. The mice then received 3×10^5 ADSCs obtained from male WT mice transduced with control dual GFP–Luciferase (Luc) or GFP-Luc-bFGF vector. These cells were injected IM adjacent to fracture sites. At day 14 post- fracture and cell transplantation, using antibody again luciferase, we observed a small number of Luc+ transplanted cells within the fracture gaps in the ADSC group (193 ± 21) and some Luc+ cells at the periphery of the callus in the ADSC^{bFGF} group (377 ± 212) (Fig. 2A, white arrows, green-stained cells). At day 21, we identified the transplanted by GFP signals. Some of the GFP+ transplanted cells were sparsely detected in the bone marrow in the ADSC group (196 ± 73) (Fig. 2B), whereas some GFP+ cells were found within bone marrow or were embedded within the callus in the ADSC^{bFGF} group (330 ± 43) (Fig. 2C). We did not detect ossification in muscle from microCT scans or in frozen sections. Transplanted cells were not detected in other tissues, as measured by quantitative real time polymerase chain reaction (qPCR) (data on file). These data suggest that some ADSCs^{bFGF} migrated to fracture gaps and were incorporated into the callus while others remained in bone marrow for at least 21 days.

Paracrine Effects of ADSC^{bFGF}

Despite the detection of only a few ADSCs^{bFGF} adjacent to the callus, endogenous osteogenesis as detected by osterix expression (red + cells) was significantly higher in ADSC^{bFGF}-treated mice as compared to ADSC-treated mice (osterix + red cells 12.6% ± 1.0% vs. 5.8 ± 1.7% in females and 10.6% ± 1.9% vs. 6.0% ± 1.8% in males) (Fig. 3A).

Because periosteal bone apposition is critical to connect fracture gaps and stabilize fractures, we were interested in identifying potential signals and/or ADSC^{bFGF}-targeted cells at the periosteal surface following ADSC^{bFGF} transplantation. Consistent with
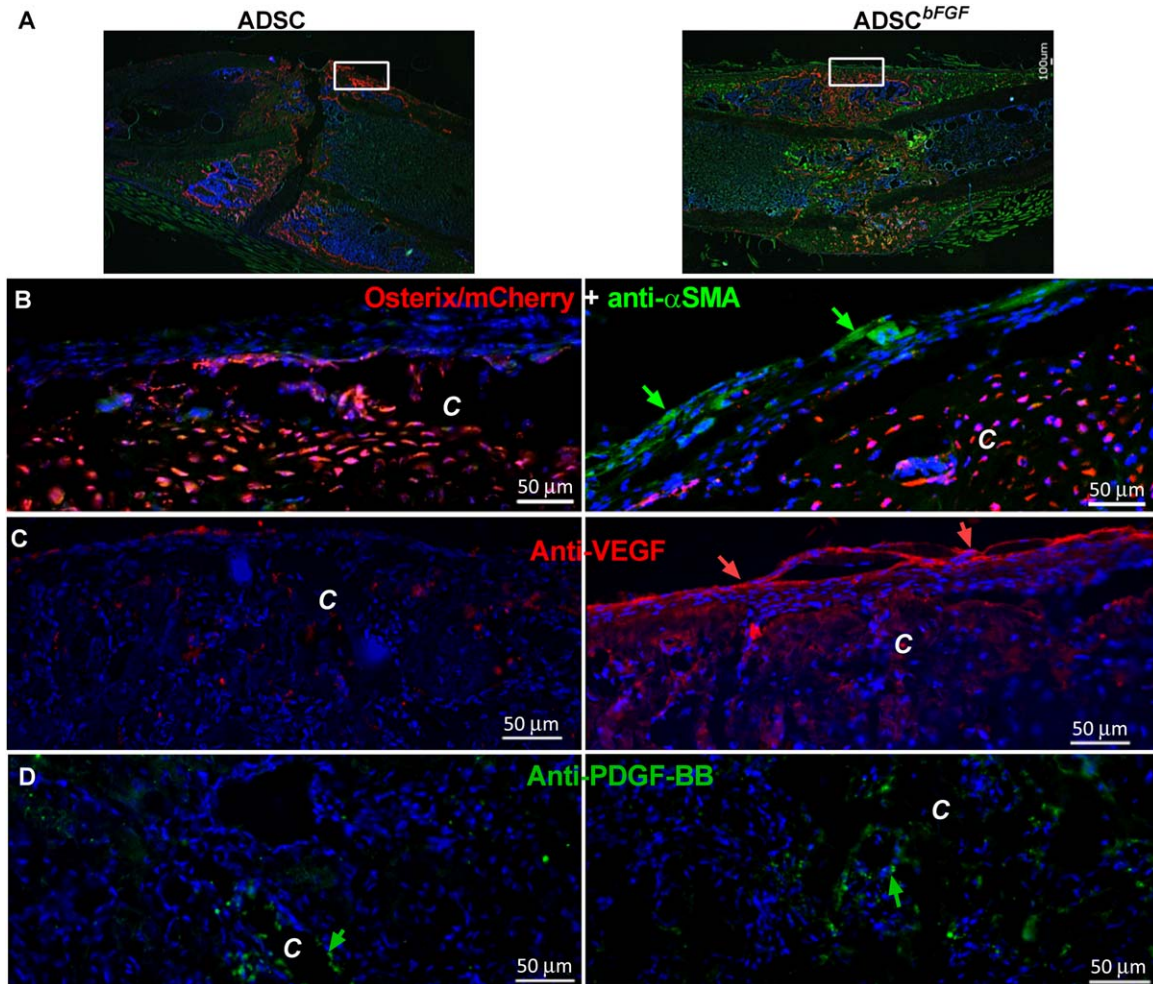
Figure 3. Paracrine signals that contributed to callus formation. Mice were treated as described in Figure 2 and sacrificed at day 14. Photos were taken from central regions of the callus (small insert to the right). Femurs were fractured in osterix-mcherry WT mice: **(A)**: low magnification showing the fractured callus. Scale bar 100 μm. **(B)**: Callus were stained with anti-αSMA conjugated to FITC (green arrows). Scale bar 50 μm. **(C)**: Fractures in osterix-mcherry WT mice were stained with anti-VEGF and Alexa-Fluo 594-conjugated secondary antibody. **(D)**: Fractures in osterix-mcherry WT mice were stained with anti-PDGF-BB and Alexa-Fluo 488-conjugated secondary antibody. Abbreviations: αSMA+, smooth muscle α–actin; ADSC, adipose-derived mouse MSCs; bFGF, basic fibroblast growth factor; C, callus; PDGF, platelet-derived growth factor PDGF; Ps, periosteal surface. Scale bar 50 μm.

previous reports [55, 56], we observed that some αSMA+ cells were present at the periosteum and periosteal surface of the callus and these cells were increased in the ADSC[bFGF] -treated group (Fig. 3B). Importantly, we observed a dramatic increase in VEGF expression, particularly at the outer periosteal region of the callus following ADSC[bFGF] treatment, suggesting endogenous activation of angiogenesis (Fig. 3C, red arrows). PDGF-BB expression was also increased in the callus surrounding sinusoid-like regions or on the periosteal bone surface (Fig. 3D, green arrows), supporting a paracrine activation of cells expressing these growth factors following ADSC[bFGF] treatment. Additionally, ADSC[bFGF] induced 2–12-fold greater expression of *Acta2* (αSMA), *Actc1* (α–CMA), *Hbegf*, *Gdf2*, and *Itgn6*, as measured q-PCR on callus tissue (data on file).

ADSC[bFGF] Increased Callus Mineralization Through Endochondral Bone Formation

We next evaluated how ADSC[bFGF] treatment affected callus bone formation and bone structure at day 21. In the female recipients, ADSC[bFGF] treatment induced 80% higher mineralizing surface and

350% higher bone formation rate than the PBS or ADSC-treated groups (Fig. 4A). In the male recipients, ADSC[bFGF] treatment induced 500% higher mineralizing surface and 750% higher bone formation rate than the PBS or ADSC-treated groups (Fig. 4B). In female recipients, ADSC[bFGF] treatment induced 56% higher total callus volume and 40% higher callus bone volume from days 21 to 35 post-fracture and treatment (Fig. 5A–5C). These morphometric changes were associated with 80% higher maximum load from days 21 and sustained at days 35 post-fracture and treatment (Fig. 5D). In male recipients, ADSC[bFGF] treatment did not affect total callus formation in comparison to PBS or ADSC-treated groups but increase callus bone volume by 13% and 23%, respectively, compared to the PBS or ADSC-treated group at days 21 and 35 post-fracture and treatment (Fig. 5E–5G). Higher mineral apposition was observed at the periosteum connecting to the fracture gaps as well as at endocortical surfaces of the pre-existing cortex that bridged the fracture gaps (black arrow heads illustrate higher mineral density color coded red) (Fig. 5F). Both maximum load and work-
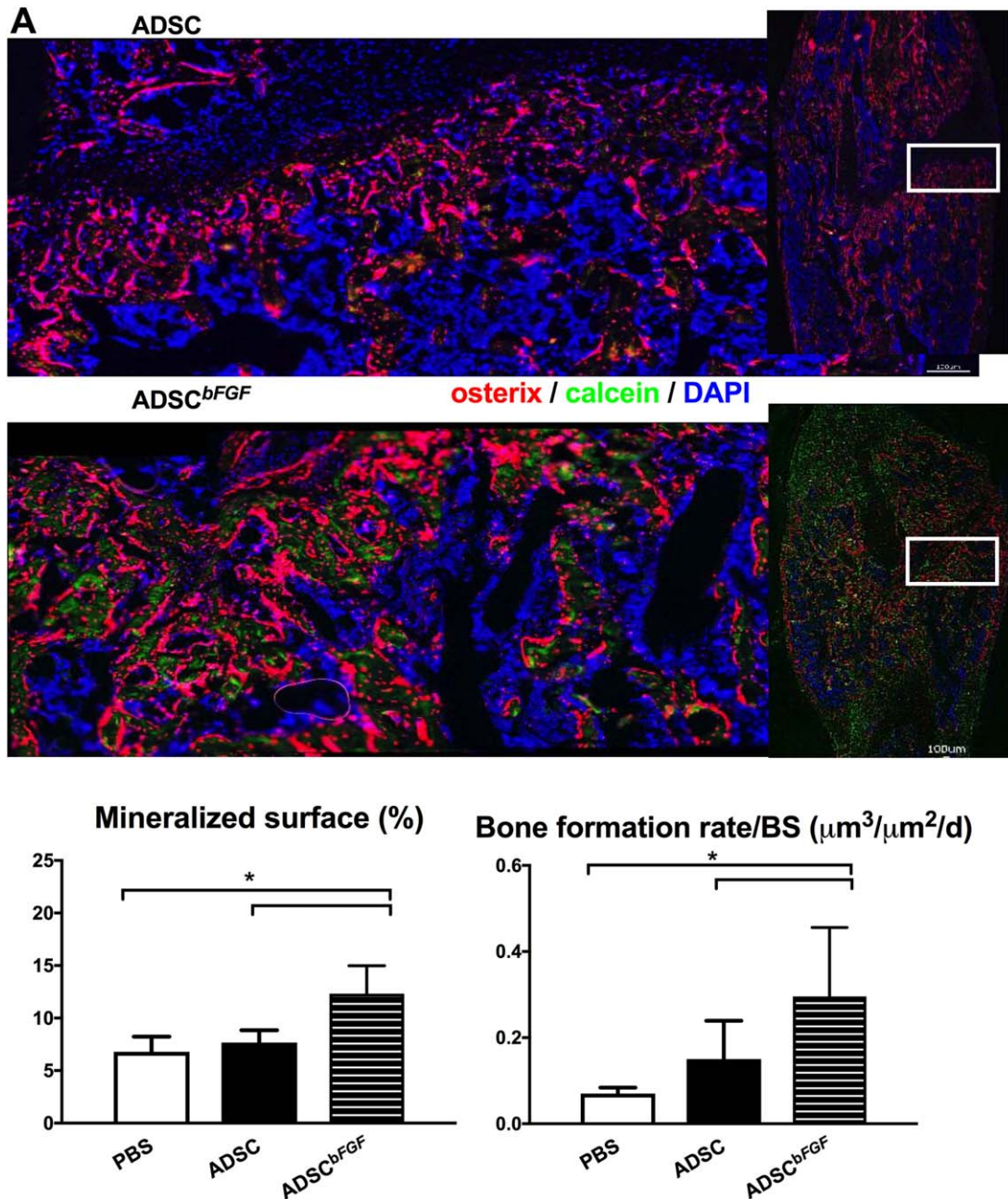
Figure 4. Bone formation at day 21. Mice were treated as described in Figure 2 and sacrificed at day 21. Calcein (10 mg/kg) was injected s.c. in mice at 9 and 2 days before sacrifice. Endogenous osterix + cells are in red and green is calcein labeling, corresponding to mineral deposition. ADSC^{bFGF} increased the green-labeled mineralized surface and bone formation rate in both the female **(A)** and male **(B)** mice. Scale bar 100 μm. *, Significant difference between indicated group by Wilcoxon ranked-sum comparison test. Abbreviations: ADSC, adipose-derived mouse MSCs; bFGF, basic fibroblast growth factor; DAPI, 4′,6-diamidino-2-phenylindole; PBS, phosphate buffered saline.

to-failure was significantly higher than PBS or ADSC-treated groups at days 35 post-fracture and treatment (Fig. 5H).

To determine whether bone formation occurred by endochondral or intramembranous bone formation mechanisms, we first crossed Col2-CreERT with Col1-GFP mice to make Col2-iCre/tdTomato mice. Then the Col2-Cre+ mice were crossed to Col12.3-GFP. Similarly, Acan-iCre-tdTomato x Col1-GFP (data on file) were generated so that we could quantitatively measure the temporal and spatial colocalization of chondrogenic cells and osteoblastic differentiation by a short course of low dose tamoxifen treatment

(3 mg/kg, i.p. × 2 days) to activate CreERT [57]. If bone formation was endochondral in nature, the Col2+ cells would populate or differentiate into osteoblasts during endochondral bone formation and become yellow. We found that most of the newly formed callus consisted of Col1+ cells (green cells, green arrow heads) that arose from the periosteal surface via intramembranous bone formation (Fig. 6). Col2+ cells (red cells, red arrows) were expressed in the growth plate and articular cartilage. These Col2+ cells seemed to be activated at the cortex, especially in the ADSC^{bFGF}-treated group. Very few Col2+ cells directly
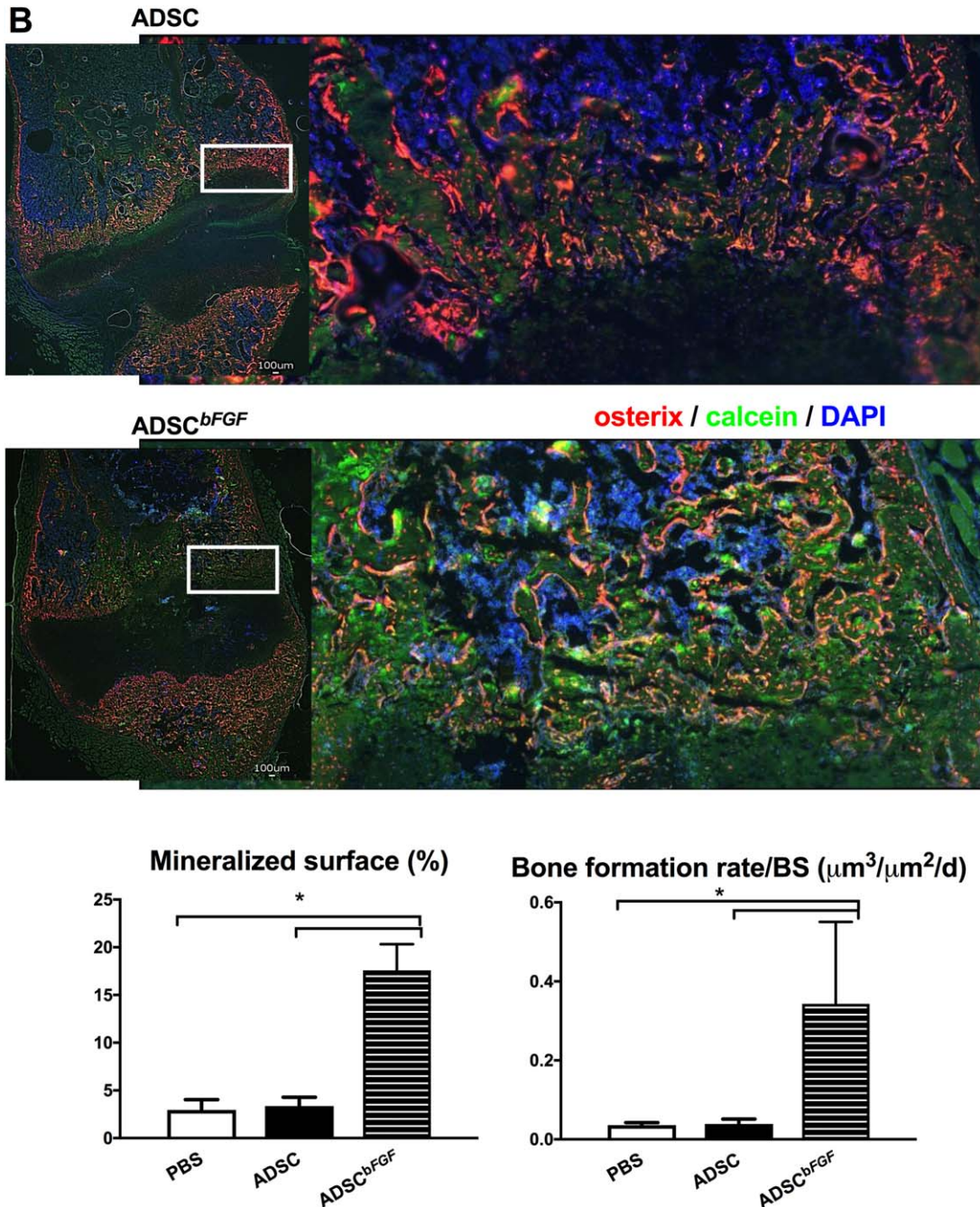
B

ADSC

ADSC[bFGF]

osterix / calcein / DAPI

Mineralized surface (%)

Bone formation rate/BS ($\mu m^3/\mu m^2/d$)

Figure 4. *Continued.*

colocalized with Col1+ osteoblasts (yellow cells). Taken together, ADSC[bFGF] treatment greatly activated Col2+ cell populations from the preexisting cortex, and these cells bridged the callus and participated in intramembrane bone formation (Fig. 6).

DISCUSSION

In the present study, we found that MSCs engineered to overexpress bFGF accelerated the fracture healing process through several mechanisms. First, some transplanted ADSC[bFGF] directly migrated to the fracture site and engrafted in the callus or within bone marrow. Although only approximately 1/1,000 of the transplanted ADSCs[bFGF] were engrafted in the fracture callus, we observed a substantial activation of endogenous angiogenesis and osteogenesis following ADSC[bFGF] transplantation, suggesting that these cells exerted most of their effects by a paracrine mechanism. Moreover, ADSC[bFGF] treatment induced a rapid conversion of soft callus to mineralized tissue resulting in higher bone mineralization and shortening the time required to regain bone strength.

The activation and migration of endogenous MSCs is critical for fracture healing in that these cells differentiate into osteoblasts and chondrocytes. The initial deposition of cartilage serves as a foundation for additional bone formation, thereby bridging fracture gaps through endochondral ossification [58]. It has been
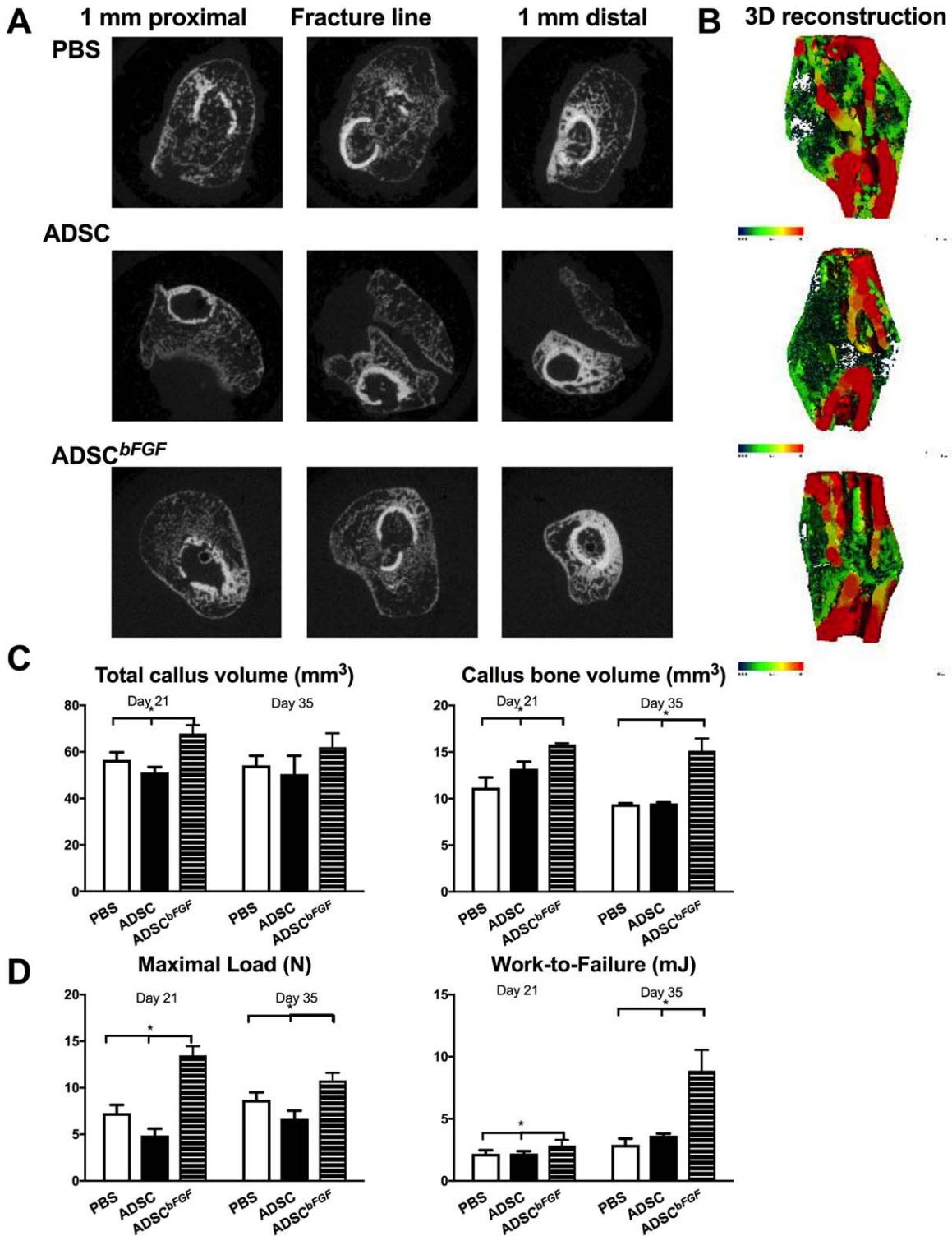
Figure 5. Callus formation and bone strength at days 21 and 35. Mice were treated as described in Figure 2 and sacrificed at days 21 or 35 post-fracture. Callus structure was first measured by microCT, then the femurs were subjected to three point-bending tests for both female **(A–D)** and male **(E–H)** mice. Representative two-dimensional images (A, E) or 3D thickness mappings (B, F) are presented for indicated groups. Red represents highly mineralized tissue, and green represents less mineralized tissue (B, F). * Significant difference between indicated group by Wilcoxon ranked-sum comparison test. Abbreviations: ADSC, adipose-derived mouse MSCs; bFGF, basic fibroblast growth factor; PBS, phosphate buffered saline.

previously demonstrated that bFGF promoted migration of MSCs in vitro [59, 60]. However, the mechanism underlying this observation is unknown. Among the endogenous osteoprogenitor cells

contributing to healing, cells expressing smooth muscle α–actin (αSMA+) and osterix (Osx+) have been identified as skeletal progenitors that give rise to osteoblasts [55, 61, 62]. Osx+ cells have
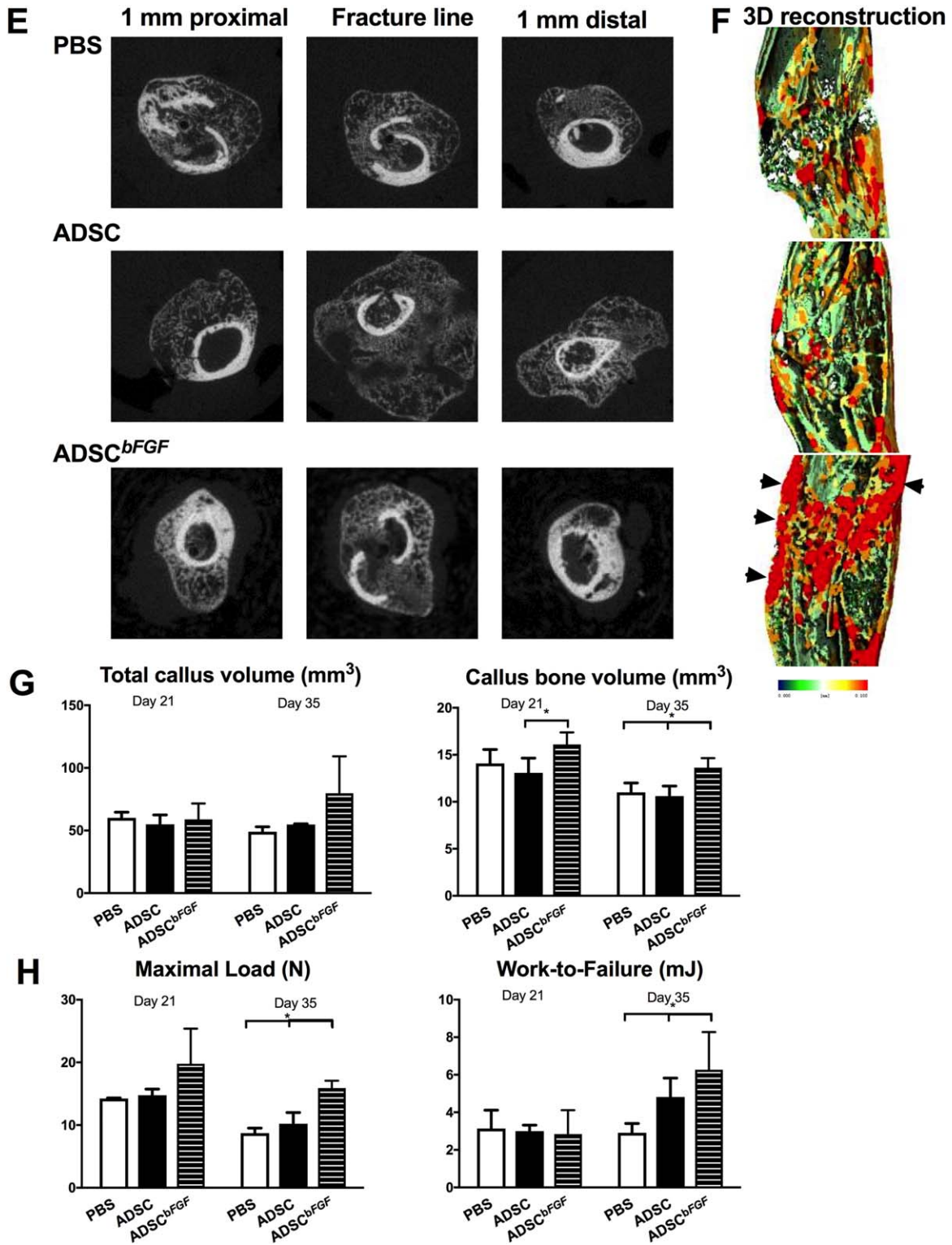
Figure 5. *Continued.*

been detected along blood vessels [62], while αSMA+ cells have been identified as mesenchymal progenitors that colocalize with newly formed bone [55] and participate in periosteal bone formation [56]. Exogenous MSC transplantation have been tested in animal models and human fractures [63]. However, it is not known whether these transplanted MSCs directly home to fracture sites and participate in the healing process, or if the MSCs release growth factors/inflammatory cytokines, thereby indirectly influencing the healing process [64–70]. The role of MSCs as immunomodulation agents during injury and tissue repair has been increasingly recognized in the field to support use of MSCs beyond simple cell replacement for diseases [71–75]. Indeed, a key
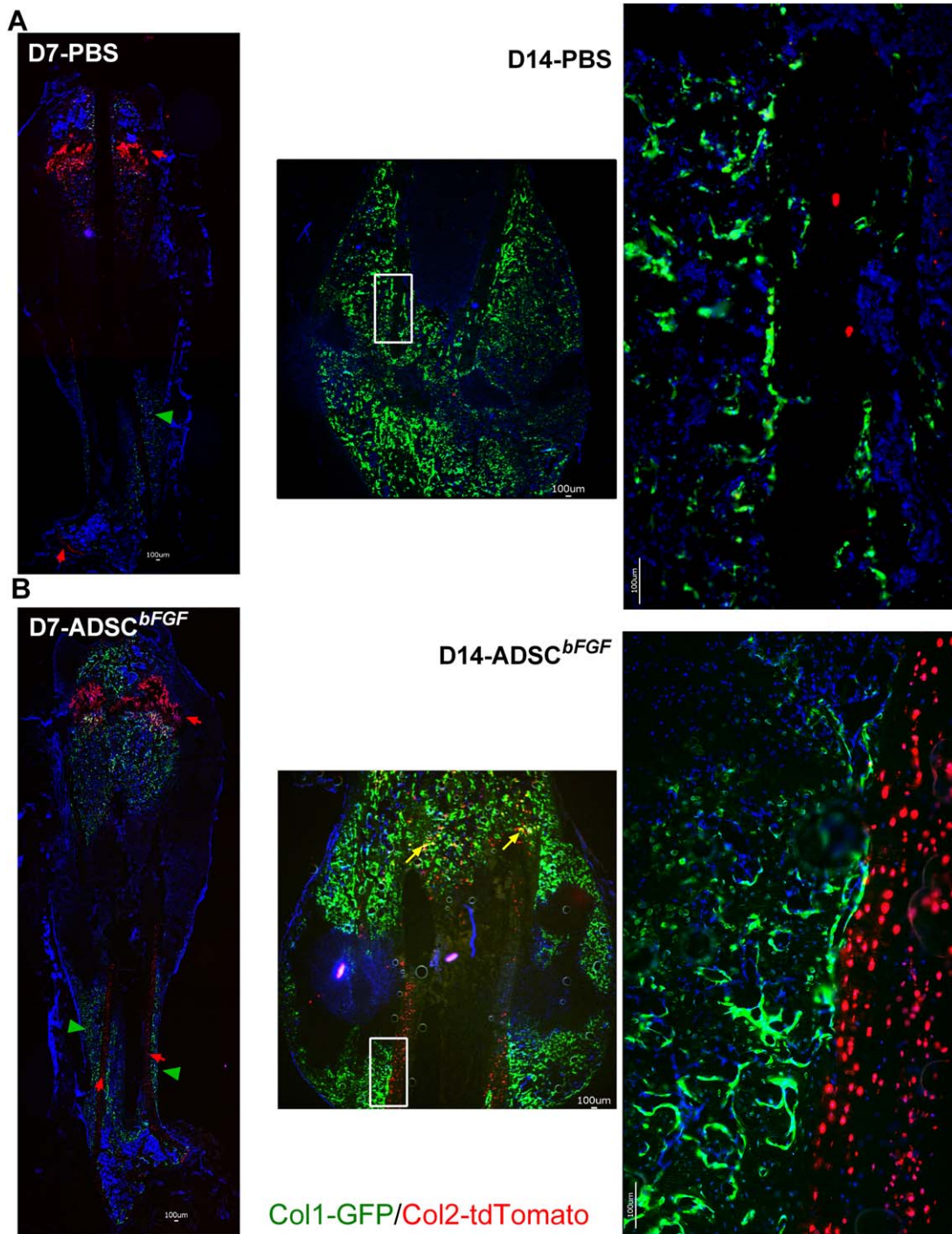
Figure 6. Effects of ADSC^bFGF treatment on chondrogenesis and osteogenesis during fracture healing. Col2-CreERT mice were crossed with tdTomato-mCherry reporter mice so that Col2+ cells and their descendants expressed tdTomato. Cre was activated by IP injection of tamoxifen (3 mg/kg × 2 days) prior to femoral fracture. Mice were sacrificed at days 7 or 14. Scale bar 100 μm. Abbreviations: ADSC, adipose-derived mouse MSCs; bFGF, basic fibroblast growth factor; PBS, phosphate buffered saline.

mechanism for MSCs to promote tissue repair is the secretion of soluble growth factors. This paracrine effect is potentially amplified when MSCs are engineered to overexpress growth factors, such as bFGF, PDGF-B, TGF-β1, and VEGF [76]. Overexpression of both bFGF and PDGF-B in MSCs increased MSC proliferation and induced a robust increase in osteogenesis. When MSCs overexpressed bFGF, we observed increased bFGF expression in MSCs.

Additionally, we observed a twofold increase in bFGF levels in the concentrated culture supernatant as well as increased VEGF levels, supporting a paracrine function for ADSC^bFGF. In vivo, we observed some ADSC^bFGF homed to the fracture gaps, but only a few cells were retained in the callus at day 21. These observations suggest that the ADSC^bFGF themselves do not directly produce a significant amount of new bone formation. However, despite only a few

ADSC^bFGF adjacent to the callus, the endogenous bone mineralization was significantly improved following ADSC^bFGF treatment, suggesting higher endogenous bone formation despite low exogenous engraftment of ADSC^bFGF. Additionally, we observed ADSC^bFGF induced higher levels of other growth factors such as *Hbegf* and *Gdf2* that were consistent with higher VEGF and PDGF-BB expression in the callus and increased angiogenesis that is essential for fracture repair [77–79].

FGF signaling is essential for postnatal chondrocyte proliferation and skeletal growth [80]. Pretreatment with bFGF during MSC expansion in vitro was key for the MSCs' trophic responses that favored bone regeneration when the cells were applied in vivo [81]. MSCs, alive or dead, were found to contain high levels of bFGF that supported neuropoiesis and angiogenesis [82]. There are two main progenitor cell components for fracture repair: cells derived from the periosteum and the surrounding soft tissue, or from the medullary area between fracture gaps [83]. However, it is difficult to precisely distinguish the contribution of various sources of progenitors during fracture healing. Our transgenic lineage tracking attempt in combination with microCT scans and histology showed that the fracture callus was initially formed from the periosteum, which was consistent with other reports [46, 53, 56, 84, 85]. ADSC^bFGF treatment showed a similar degree of bone formation from the periosteal surface. ADSC^bFGF induced the early activation of collagen 2 at the fractured ends of the cortex which promoted both chondrogenesis and osteogenesis. There was a rapid transition from a big, soft callus to union with highly mineralized callus from internal ossification which may have significantly contributed to stabilization of the fracture and improved bone strength following ADSC^bFGF treatment. Some reports suggested that direct descendants of chondrocytes become osteocytes as part of endochondral bone formation [86–90]. Our study showed very few chondrocyte-lineage cells (marked by collagen-2 or aggrecan) colocalized with osteoblasts (marked by collagen-1). This finding indicates a minor role for direct differentiation of chondrocytes to osteoblasts during normal healing or following ADSC^bFGF treatment.

We and others have found that bFGF injections for two weeks induced profound de novo new bone formation [25, 26]. To explore the potential application of bFGF as an anabolic treatment for bone, we used a severely osteopenia rat model at 120 days post-ovariectomy. The effects of bFGF on trabecular bone architecture, osteoblast activity, and bone strength were compared to those of hPTH (1-34). We found that treatment of OVX rats with bFGF or hPTH (1-34) for 6 weeks both increased trabecular bone mass, but hPTH (1-34) increased trabecular thickness whereas bFGF increased trabecular number and connectivity [38–40]. Transgenic mice overexpressing bFGF had higher levels of osteoblast maturation and vascular invasion during the early fracture repair period [24]. Previous studies have shown that short-term bFGF injection induces profound de novo bone formation in rodents [25, 26]. Basic FGF stimulates blood vessel growth and has synergetic effects with vascular endothelial growth factor (VEGF) and platelet-derived growth factor (PDGF) during angiogenesis, which are important for wound healing [27, 91, 92]. Similar to BMPs, bFGF peptide is injected directly or loaded in a scaffold to promote fracture healing [28–31] or for periodontal regeneration [93–95]. One injection of bFGF recombinant protein directly at the fracture site increased callus formation and bone mechanical strength in normal and streptozotocin-diabetic rats [96]. Although injections with bFGF peptide typically increase early osteoprogenitor cell proliferation, stimulate bone formation, and induce larger calluses compared with controls, whether this treatment improves bone mechanical strength remains to be determined [22, 32–34]. Moreover, prolonged exposure to protein mitogens, such as FGFs, is associated with increased risk for cancer [35–37] and induces pro-inflammatory responses in vitro [97]. The oncogenic and proinflammatory effects of bFGF were observed with continuous exposure to bFGF at the dose of 10ng/mL or greater, which were approximately at least 1,000-fold higher than the level of bFGF being released from MSCs. Additionally, systemic bFGF injection also can induce severe anemia and shift the fate of progenitor cells toward an osteoblast lineage at the expense of the hematopoietic lineage, thereby limiting systemic application of this growth factor [38, 39]. However, we found that one local injection of MSC^bFGF resulted in short-term release of bFGF and other growth factors, such as VEGF, that augmented angiogenesis, improved bone apposition and expedited the recovery of bone strength, which might serve as an alternative treatment option for fracture repair.

Although we used MSCs engineered to express bFGF for fracture healing in this study, it is important to note that MSCs engineered to express other growth factors, such as IGF-1, BMPs or VEGF, have also exhibited beneficial effects on bone regeneration [41–43]. We elected to focus on bFGF since MSCs overexpressing bFGF only mildly affects adipogenesis, which was markedly inhibited by MSCs overexpressing PDGF-B. Overexpression of TGF-β1 in MSCs blocked both osteogenic and adipogenic differentiation. MSCs engineered to overexpress VEGF induced migration of endothelial cells and did not differ from controls in osteogenic or adipogenic differentiation, likely reflecting a lack of VEGF receptor expression on MSCs [76]. Taken together, MSCs overexpressing bFGF are superior to MSCs expressing other growth factors such as TGF-β1 and VEGF in terms of osteogenic potential and have the least effect on adipogenesis or morphological changes in MSCs in vitro. Appropriate levels of both bFGF and VEGF are critical for osteogenesis, and too much bFGF, VEGF, or TGF-β1 resulted in impaired mineralization [30, 39, 98–101]. Our data suggest that bFGF secretion from cells was sustained for up to 7 days, and the transplanted cells were retained in the callus within bone marrow for up to 21 days. These findings indicate that the potential therapeutic window for effective MSC^bFGF use is approximately one-two weeks. Since MSCs tend to home to sites of inflammation [58], we chose intramuscular injection instead of intravenous injection to avoid cells being trapped in the lung. However, this approach may increase the risk for extra-skeletal ossification in the muscle. One other potential route of application would be intraosseous injection, which maybe technically more challenging, but may increase cell retention in the fracture site and reduce the risk for extra-skeletal ossification. We used MSC in doses of 100,000–3,000,000 cells and conclude that there was no dose dependent effects of cell numbers engrafting to callus. Therefore, there was no dose dependent effect for increasing cell numbers in this model. This finding are similar to the results of a clinical study in which recombinant human bFGF was used to treated tibia-fractures in 70 human subjects. There was no difference in fracture union by radiologic assessments between the high (2.4 mg) and low (0.8 mg) doses, both of which were better treatments compared to placebo [30]. Nevertheless, the optimal dose for ADSC^bFGF, the time of initial treatment,

duration of treatment, and delivery methods require further investigation.

Sex significantly affected the healing process [102–106]. MSCs derived from bone marrow obtained from young male mice have higher doubling times than that of their aged-matched female-derived counterparts [105]. Muscle-derived stem cells (MDSCs) obtained from male donors displayed more osteogenic and chondrogenic potential than those obtained from female donors [107, 108]. Sex also affected the regenerative capacity of MSCs [102, 104]. We found that MSCs derived from male mice had higher osteogenic potential [51] and that male mice generally formed bigger callus than the aged-matched females (Fig. 5) [46]. However, despite the intrinsic sex differences in fracture repair, effects of MSC^{bFGF} on remodeling of the soft callus into mineralized callus and on bone strength were sex-independent.

CONCLUSION

There were multiple beneficial effects for use of ADSC^{bFGF} for fracture repair: first, as a direct MSCs supplement; secondly, ADSC^{bFGF} stimulated trophic factors such as bFGF, VEGF, and PDGF that stimulate angiogenesis, osteoblast differentiation, and bone formation at the fracture site; and thirdly, ADSC^{bFGF} induced a rapid cartilage turnover through endochondral ossification and enhances bone strength. Taken together, ADSC^{bFGF} may serve as a potential cell-based treatment for fracture repair as it can provide an environment rich in stem cells, growth factors, and bone matrix proteins over a short time period, which can promote bone regeneration.

AUTHOR CONTRIBUTIONS

A.K.: collection and assembly of data, data analysis and interpretation, manuscript writing and final approval of manuscript; H.L.Z.: collection and assembly of data, data analysis and interpretation, and final approval of manuscript; E.A.Y. and F.F.: collection and assembly of data, data analysis, and final approval of manuscript; H.L.C.: collection and assembly of data, data analysis and final approval of manuscript; N.E.L.: study design data analysis and interpretation, and final approval of manuscript; W.Y.: conception and design, collection and assembly of data, data analysis and interpretation, manuscript writing and final approval of manuscript.

REFERENCES

1 Maciejewski ML, Radcliff TA, Henderson WG et al. Determinants of postsurgical discharge setting for male hip fracture patients. J Rehabil Res Dev 2013;50:1267–1276.

2 Kaback LA, Soung do Y, Naik A et al. Teriparatide (1–34 human PTH) regulation of osterix during fracture repair. J Cell Biochem 2008;105:219–226.

3 Alkhiary YM, Gerstenfeld LC, Krall E et al. Enhancement of experimental fracture-healing by systemic administration of recombinant human parathyroid hormone (PTH 1–34). J Bone Joint Surg Am 2005;87:731–741.

4 Yukata K, Xie C, Li TF et al. Aging periosteal progenitor cells have reduced regenerative responsiveness to bone injury and to the anabolic actions of PTH 1–34 treatment. Bone 2014;62:79–89.

5 Zhang D, Potty A, Vyas P et al. The role of recombinant PTH in human fracture healing: A systematic review. J Orthop Trauma 2014;28:57–62.

6 Nakamura T, Sugimoto T, Nakano T et al. Randomized Teriparatide [human parathyroid hormone (PTH) 1–34] Once-Weekly Efficacy Research (TOWER) trial for examining the reduction in new vertebral fractures in subjects with primary osteoporosis and high fracture risk. J Clin Endocrinol Metab 2012;97:3097–3106.

7 Cipriano CA, Issack PS, Shindle L et al. Recent advances toward the clinical application of PTH (1–34) in fracture healing. HSS J 2009;5:149–153.

8 Lee FY, Storer S, Hazan EJ et al. Repair of bone allograft fracture using bone morphogenetic protein-2. Clin Orthop Relat Res 2002:119–126.

9 Govender S, Csimma C, Genant HK et al. Recombinant human bone morphogenetic protein-2 for treatment of open tibial fractures: A prospective, controlled, randomized study of four hundred and fifty patients. J Bone Joint Surg Am 2002;84-A:2123–2134.

10 Calori GM, Tagliabue L, Gala L et al. Application of rhBMP-7 and platelet-rich plasma in the treatment of long bone non-unions: A prospective randomised clinical study on 120 patients. Injury 2008;39:1391–1402.

11 Katayama Y, Matsuyama Y, Yoshihara H et al. Clinical and radiographic outcomes of posterolateral lumbar spine fusion in humans using recombinant human bone morphogenetic protein-2: An average five-year follow-up study. Int Orthop 2009;33:1061–1067.

12 Jones AL, Bucholz RW, Bosse MJ et al. Recombinant human BMP-2 and allograft compared with autogenous bone graft for reconstruction of diaphyseal tibial fractures with cortical defects. A randomized, controlled trial. J Bone Joint Surg Am 2006;88:1431–1441.

13 Friedlaender GE, Perry CR, Cole JD et al. Osteogenic protein-1 (bone morphogenetic protein-7) in the treatment of tibial nonunions. J Bone Joint Surg Am 2001;83-A(suppl 1):S151–158.

14 White AP, Vaccaro AR, Hall JA et al. Clinical applications of BMP-7/OP-1 in fractures, nonunions and spinal fusion. Int Orthop 2007;31:735–741.

15 Yilgor P, Hasirci N, Hasirci V. Sequential BMP-2/BMP-7 delivery from polyester nanocapsules. J Biomed Mater Res A 2010;93:528–536.

16 Mines D, Gu Y, Kou TD et al. Recombinant human bone morphogenetic protein-2 and pancreatic cancer: A retrospective cohort study. Pharmacoepidemiol Drug Saf 2011;20:111–118.

17 Spiro AS, Beil FT, Schinke T et al. Short-term application of dexamethasone enhances bone morphogenetic protein-7-induced ectopic bone formation in vivo. J Trauma 2010;69:1473–1480.

18 Spiro AS, Beil FT, Baranowsky A et al. BMP-7-induced ectopic bone formation and fracture healing is impaired by systemic NSAID application in C57BL/6-mice. J Orthop Res 2010;28:785–791.

19 Pacicca DM, Patel N, Lee C et al. Expression of angiogenic factors during distraction osteogenesis. Bone 2003;33:889–898.

20 Haque T, Amako M, Nakada S et al. An immunohistochemical analysis of the temporal and spatial expression of growth factors FGF 1, 2 and 18, IGF 1 and 2, and TGFbeta1 during distraction osteogenesis. Histol Histopathol 2007;22:119–128.

21 Schmid GJ, Kobayashi C, Sandell LJ et al. Fibroblast growth factor expression during skeletal fracture healing in mice. Dev Dyn 2009;238:766–774.

22 Nakajima F, Ogasawara A, Goto K et al. Spatial and temporal gene expression in chondrogenesis during fracture healing and the effects of basic fibroblast growth factor. J Orthop Res 2001;19:935–944.

23 Takechi M, Tatehara S, Satomura K et al. Effect of FGF-2 and melatonin on implant bone healing: A histomorphometric study. J Mater Sci Mater Med 2008;19:2949–2952.

24 Hurley MM, Adams DJ, Wang L et al. Accelerated fracture healing in transgenic mice overexpressing an anabolic isoform of fibroblast growth factor 2. J Cell Biochem 2015;117:599–611.

25 Lane NE, Yao W, Kinney JH et al. Both hPTH(1-34) and bFGF increase trabecular bone mass in osteopenic rats but they have different effects on trabecular bone architecture. J Bone Miner Res 2003;18:2105–2115.

26 Lane NE, Kumer J, Yao W et al. Basic fibroblast growth factor forms new trabeculae that physically connect with pre-existing trabeculae, and this new bone is maintained with an anti-resorptive agent and enhanced with an anabolic agent in an osteopenic rat model. Osteoporos Int 2003;14:374–382.

27 Cao R, Brakenhielm E, Pawliuk R et al. Angiogenic synergism, vascular stability and improvement of hind-limb ischemia by a combination of PDGF-BB and FGF-2. Nat Med 2003;9:604–613.

28 Nakamura T, Hara Y, Tagawa M et al. Recombinant human basic fibroblast growth factor accelerates fracture healing by enhancing callus remodeling in experimental dog tibial fracture. J Bone Miner Res 1998;13:942–949.

29 Kawaguchi H, Jingushi S, Izumi T et al. Local application of recombinant human fibroblast growth factor-2 on bone repair: A dose-escalation prospective trial on patients with osteotomy. J Orthop Res 2007;25:480–487.

30 Kawaguchi H, Oka H, Jingushi S et al. A local application of recombinant human fibroblast growth factor 2 for tibial shaft fractures: A randomized, placebo-controlled trial. J Bone Miner Res 2010;25:2735–2743.

31 Maehara H, Sotome S, Yoshii T et al. Repair of large osteochondral defects in rabbits using porous hydroxyapatite/collagen (HAp/Col) and fibroblast growth factor-2 (FGF-2). J Orthop Res 2010 28:677–686.

32 van Gastel N, Stegen S, Stockmans I et al. Expansion of murine periosteal progenitor cells with fibroblast growth factor 2 reveals an intrinsic endochondral ossification program mediated by bone morphogenetic protein 2. Stem Cells 2014;32:2407–2418.

33 Bland YS, Critchlow MA, Ashhurst DE. Exogenous fibroblast growth factors-1 and −2 do not accelerate fracture healing in the rabbit. Acta Orthop Scand 1995;66:543–548.

34 Nakajima F, Nakajima A, Ogasawara A et al. Effects of a single percutaneous injection of basic fibroblast growth factor on the healing of a closed femoral shaft fracture in the rat. Calcif Tissue Int 2007;81:132–138.

35 Marek LA, Hinz TK, von Massenhausen A et al. Nonamplified FGFR1 is a growth driver in malignant pleural mesothelioma. Mol Cancer Res 2014;12:1460–1469.

36 Piperdi B, Merla A, Perez-Soler R. Targeting angiogenesis in squamous non-small cell lung cancer. Drugs 2014;74:403–413.

37 Terai H, Soejima K, Yasuda H et al. Activation of the FGF2-FGFR1 autocrine pathway: A novel mechanism of acquired resistance to gefitinib in NSCLC. Mol Cancer Res 2013;11:759–767.

38 Iwaniec UT, Moore K, Rivera MF et al. A comparative study of the bone-restorative efficacy of anabolic agents in aged ovariectomized rats. Osteoporos Int 2007;18:351–362.

39 Yao W, Hadi T, Jiang Y et al. Basic fibroblast growth factor improves trabecular bone connectivity and bone strength in the lumbar vertebral body of osteopenic rats. Osteoporos Int 2005;16:1939–1947.

40 Yao W, Balooch G, Balooch M et al. Sequential treatment of ovariectomized mice with bFGF and risedronate restored trabecular bone microarchitecture and mineralization. Bone 2006;39:460–469.

41 Granero-Molto F, Myers TJ, Weis JA et al. Mesenchymal stem cells expressing insulin-like growth factor-I (MSCIGF) promote fracture healing and restore new bone formation in Irs1 knockout mice: Analyses of MSCIGF autocrine and paracrine regenerative effects. Stem Cells 2011;29:1537–1548.

42 Gamradt SC, Lieberman JR. Genetic modification of stem cells to enhance bone repair. Ann Biomed Eng 2004;32:136–147.

43 Tai K, Pelled G, Sheyn D et al. Nanobiomechanics of repair bone regenerated by genetically modified mesenchymal stem cells. Tissue Eng Part A 2008;14:1709–1720.

44 Manigrasso MB, O'Connor JP. Characterization of a closed femur fracture model in mice. J Orthop Trauma 2004;18:687–695.

45 Holstein JH, Matthys R, Histing T et al. Development of a stable closed femoral fracture model in mice. J Surg Res 2009;153:71–75.

46 Yao W, Lay YE, Kot A et al. Improved mobilization of exogenous mesenchymal stem cells to bone for fracture healing and sex difference. Stem Cells 2016;34:2587–2600.

47 Freeman TA, Patel P, Parvizi J et al. Micro-CT analysis with multiple thresholds allows detection of bone formation and resorption during ultrasound-treated fracture healing. J Orthop Res 2009;27:673–679.

48 Dempster DW, Compston JE, Drezner MK et al. Standardized nomenclature, symbols, and units for bone histomorphometry: A 2012 update of the report of the ASBMR Histomorphometry Nomenclature Committee. J Bone Miner Res 2013;28:2–17.

49 Yao W, Cheng Z, Shahnazari M et al. Overexpression of secreted frizzled-related protein 1 inhibits bone formation and attenuates parathyroid hormone bone anabolic effects. J Bone Miner Res 2010;25:190–199.

50 Yao W, Guan M, Jia J et al. Reversing bone loss by directing mesenchymal stem cells to bone. Stem Cells 2013;31:2003–2014.

51 Yao W, Dai W, Shahnazari M et al. Inhibition of the progesterone nuclear receptor during the bone linear growth phase increases peak bone mass in female mice. PLoS One 2010;5:e11410.

52 Nishimura R, Wakabayashi M, Hata K et al. Osterix regulates calcification and degradation of chondrogenic matrices through matrix metalloproteinase 13 (MMP13) expression in association with transcription factor Runx2 during endochondral ossification. J Biol Chem 2012;287:33179–33190.

53 Mizoguchi T, Pinho S, Ahmed J et al. Osterix marks distinct waves of primitive and definitive stromal progenitors during bone marrow development. Dev Cell 2014;29:340–349.

54 Liu Y, Strecker S, Wang L et al. Osterix-cre labeled progenitor cells contribute to the formation and maintenance of the bone marrow stroma. PLoS One 2013;8:e71318.

55 Grcevic D, Pejda S, Matthews BG et al. In vivo fate mapping identifies mesenchymal progenitor cells. Stem Cells 2012;30:187–196. [PMC][10.1002/stem.780] [22083974]

56 Ushiku C, Adams DJ, Jiang X et al. Long bone fracture repair in mice harboring GFP reporters for cells within the osteoblastic lineage. J Orthop Res 2010;28:1338–1347.

57 Zhong ZA, Sun W, Chen H et al. Optimizing tamoxifen-inducible Cre/loxp system to reduce tamoxifen effect on bone turnover in long bones of young mice. Bone 2015;81:614–619.

58 Hadjiargyrou M, O'Keefe RJ. The convergence of fracture repair and stem cells: Interplay of genes, aging, environmental factors and disease. J Bone Miner Res 2014;29:2307–2322.

59 Schmidt A, Ladage D, Schinkothe T et al. Basic fibroblast growth factor controls migration in human mesenchymal stem cells. Stem Cells 2006;24:1750–1758.

60 Latifi-Pupovci H, Kuci Z, Wehner S et al. In vitro migration and proliferation ("wound healing") potential of mesenchymal stromal cells generated from human CD271(+) bone marrow mononuclear cells. J Transl Med 2015;13:315.

61 Kinner B, Pacicca DM, Gerstenfeld LC et al. Expression of smooth muscle actin in cells involved in distraction osteogenesis in a rat model. J Orthop Res 2003;21:20–27.

62 Maes C, Kobayashi T, Selig MK et al. Osteoblast precursors, but not mature osteoblasts, move into developing and fractured bones along with invading blood vessels. Dev Cell 2010;19:329–344.

63 Gomez-Barrena E, Rosset P, Lozano D et al. Bone fracture healing: Cell therapy in delayed unions and nonunions. Bone 2015;70:93–101.

64 Kawano S, Otsu K, Kuruma A et al. ATP autocrine/paracrine signaling induces calcium oscillations and NFAT activation in human mesenchymal stem cells. Cell Calcium 2006;9:313–324.

65 Mayer H, Bertram H, Lindenmaier W et al. Vascular endothelial growth factor (VEGF-A) expression in human mesenchymal stem cells: Autocrine and paracrine role on osteoblastic and endothelial differentiation. J Cell Biochem 2005;95:827–839.

66 Kim J, Ma T. Autocrine fibroblast growth factor 2-mediated interactions between human mesenchymal stem cells and the extracellular matrix under varying oxygen tension. J Cell Biochem 2013;114:716–727.

67 Briolay A, Lencel P, Bessueille L et al. Autocrine stimulation of osteoblast activity by Wnt5a in response to TNF-alpha in human mesenchymal stem cells. Biochem Biophys Res Commun 2013;430:1072–1077.

68 Bastiaans J, van Meurs JC, van Holten-Neelen C et al. Thrombin induces epithelial-mesenchymal transition and collagen production by retinal pigment epithelial cells via autocrine PDGF-receptor signaling. Invest Ophthalmol Vis Sci 2013;54:8306–8314.

69 Alcaraz A, Mrowiec A, Insausti CL et al. Autocrine TGF-beta induces epithelial to

mesenchymal transition in human amniotic epithelial cells. Cell Transplant 2013;22:1351–1367.

70 Fruscione F, Scarfi S, Ferraris C et al. Regulation of human mesenchymal stem cell functions by an autocrine loop involving NAD+ release and P2Y11-mediated signaling. Stem Cells Dev 2011;20:1183–1198.

71 Bianco P, Cao X, Frenette PS et al. The meaning, the sense and the significance: Translating the science of mesenchymal stem cells into medicine. Nat Med 2013;19:35–42.

72 Gazdic M, Volarevic V, Arsenijevic N et al. Mesenchymal stem cells: A friend or foe in immune-mediated diseases. Stem Cell Rev 2015;11:280–287.

73 Boregowda SV, Phinney DG. MSCs: Paracrine effects. Mesenchymal Stromal Cells 2013;145–167.

74 Keating A. Mesenchymal stromal cells: New directions. Cell Stem Cell 2012;10:709–716.

75 Murphy MB, Moncivais K, Caplan AI. Mesenchymal stem cells: Environmentally responsive therapeutics for regenerative medicine. Exp Mol Med 2013;45:e54.

76 Fierro FA, Kalomoiris S, Sondergaard CS et al. Effects on proliferation and differentiation of multipotent bone marrow stromal cells engineered to express growth factors for combined cell and gene therapy. Stem Cells 2011; 29:1727–1737.

77 Duvall CL, Taylor WR, Weiss D et al. Impaired angiogenesis, early callus formation, and late stage remodeling in fracture healing of osteopontin-deficient mice. J Bone Miner Res 2007;22:286–297.

78 Tomlinson RE, McKenzie JA, Schmieder AH et al. Angiogenesis is required for stress fracture healing in rats. Bone 2013;52:212–219.

79 Wang CY, Yang HB, Hsu HS et al. Mesenchymal stem cell-conditioned medium facilitates angiogenesis and fracture healing in diabetic rats. J Tissue Eng Regen Med 2012;6:559–569.

80 Karuppaiah K, Yu K, Lim J et al. FGF signaling in the osteoprogenitor lineage non-autonomously regulates postnatal chondrocyte proliferation and skeletal growth. Development 2016;143:1811–1822.

81 Tasso R, Gaetani M, Molino E et al. The role of bFGF on the ability of MSC to activate endogenous regenerative mechanisms in an ectopic bone formation model. Biomaterials 2012;33:2086–2096.

82 Aizman I, Vinodkumar D, McGrogan M et al. Cell injury-induced release of FGF2: Relevance to intracerebral mesenchymal stromal cell transplantations. Stem Cells Dev 2015;24:1623–1634.

83 Einhorn TA, Gerstenfeld LC. Fracture healing: Mechanisms and interventions. Nat Rev Rheumatol 2015;11:45–54.

84 Kalajzic Z, Li H, Wang LP et al. Use of an alpha-smooth muscle actin GFP reporter to identify an osteoprogenitor population. Bone 2008;43:501–510.

85 Grcevic D, Pejda S, Matthews BG et al. In vivo fate mapping identifies mesenchymal progenitor cells. Stem Cells 2012;30:187–196.

86 Kahn AJ, Simmons DJ. Chondrocyte-to-osteocyte transformation in grafts of perichondrium-free epiphyseal cartilage. Clin Orthop Relat Res 1977;129:299–304.

87 Roach HI. Trans-differentiation of hypertrophic chondrocytes into cells capable of producing a mineralized bone matrix. Bone Miner 1992;19:1–20.

88 Park J, Gebhardt M, Golovchenko S et al. Dual pathways to endochondral osteoblasts: A novel chondrocyte-derived osteoprogenitor cell identified in hypertrophic cartilage. Biol Open 2015;4:608–621.

89 Tsang KY, Chan D, Cheah KS. Fate of growth plate hypertrophic chondrocytes: Death or lineage extension? Dev Growth Differ 2015;57:179–192.

90 Ono N, Ono W, Nagasawa T et al. A subset of chondrogenic cells provides early mesenchymal progenitors in growing bones. Nat Cell Biol 2014;16:1157–1167.

91 Motokawa M, Kaku M, Matsuda Y et al. Effects of occlusal hypofunction and its recovery on PDL structure and expression of VEGF and bFGF in rats. Clin Oral Investig 2015;19:929–935.

92 Saito W, Uchida K, Matsushita O et al. Acceleration of callus formation during fracture healing using basic fibroblast growth factor-kidney disease domain-collagen-binding domain fusion protein combined with allogenic demineralized bone powder. J Orthop Surg Res 2015;10:59.

93 Kitamura M, Akamatsu M, Kawanami M et al. Randomized placebo-controlled and controlled non-inferiority phase iii trials comparing trafermin, a recombinant human fibroblast growth factor 2, and enamel matrix derivative in periodontal regeneration in intrabony defects. J Bone Miner Res 2016;31:806–814.

94 Murakami S, Takayama S, Kitamura M et al. Recombinant human basic fibroblast growth factor (bFGF) stimulates periodontal regeneration in class II furcation defects created in beagle dogs. J Periodontal Res 2003;38:97–103.

95 Takayama S, Murakami S, Shimabukuro Y et al. Periodontal regeneration by FGF-2 (bFGF) in primate models. J Dent Res 2001;80:2075–2079.

96 Kawaguchi H, Kurokawa T, Hanada K et al. Stimulation of fracture repair by recombinant human basic fibroblast growth

factor in normal and streptozotocin-diabetic rats. Endocrinology 1994;135:774–781.

97 Ben Jemaa A, Sallami S, Ramarli D et al. The proinflammatory cytokine, IL-6, and its interference with bFGF signaling and PSMA in prostate cancer cells. Inflammation 2013;36:643–650.

98 Kuhn LT, Ou G, Charles L et al. Fibroblast growth factor-2 and bone morphogenetic protein-2 have a synergistic stimulatory effect on bone formation in cell cultures from elderly mouse and human bone. J Gerontol A Biol Sci Med Sci 2013;68:1170–1180.

99 Liang H, Pun S, Wronski TJ. Bone anabolic effects of basic fibroblast growth factor in ovariectomized rats. Endocrinology 1999;140:5780–5788.

100 Hu K, Olsen BR. Osteoblast-derived VEGF regulates osteoblast differentiation and bone formation during bone repair. J Clin Invest 2016;126:509–526.

101 Kassem M, Kveiborg M, Eriksen EF. Production and action of transforming growth factor-beta in human osteoblast cultures: Dependence on cell differentiation and modulation by calcitriol. Eur J Clin Invest 2000;30:429–437.

102 Gao X, Usas A, Proto JD et al. Role of donor and host cells in muscle-derived stem cell-mediated bone repair: Differentiation vs. paracrine effects. FASEB J 2014;28:3792–3809.

103 Deasy BM, Schugar RC, Huard J. Sex differences in muscle-derived stem cells and skeletal muscle. Crit Rev Eukaryot Gene Exp 2008;18:173–188.

104 Meszaros LB, Usas A, Cooper GM et al. Effect of host sex and sex hormones on muscle-derived stem cell-mediated bone formation and defect healing. Tissue Eng Part A 2012;18:1751–1759.

105 Katsara O, Mahaira LG, Iliopoulou EG et al. Effects of donor age, gender, and in vitro cellular aging on the phenotypic, functional, and molecular characteristics of mouse bone marrow-derived mesenchymal stem cells. Stem Cells Dev 2011;20:1549–1561.

106 Crisostomo PR, Wang M, Herring CM et al. Gender differences in injury induced mesenchymal stem cell apoptosis and VEGF, TNF, IL-6 expression: Role of the 55 kDa TNF receptor (TNFR1). J Mol Cell Cardiol 2007;42:142–149.

107 Matsumoto T, Kubo S, Meszaros LB et al. The influence of sex on the chondrogenic potential of muscle-derived stem cells: Implications for cartilage regeneration and repair. Arthritis Rheum 2008;58:3809–3819.

108 Corsi KA, Pollett JB, Phillippi JA et al. Osteogenic potential of postnatal skeletal muscle-derived stem cells is influenced by donor sex. J Bone Miner Res 2007;22:1592–1602.